UNIVERSIDADE DE SÃO PAULO

PUBLICAÇÕES

IFUSP/P-673

BOSE-EINSTEIN CORRELATION OF PARTICLES PRODUCED BY EXPANDING SOURCES

Y. Hama and Sandra S. Padula

Instituto de Física, Universidade de São Paulo

BOSE-EINSTEIN CORRELATION OF PARTICLES PRODUCED BY EXPANDING SOURCES

Y. Hama and Sandra S. Padula

Instituto de Física, Universidade de São Paulo
São Paulo, Brasil

ABSTRACT

Bose-Einstein correlation is discussed for par-
ticles produced by rapidly expanding sources,
when kinematical effects hinder a direct rela-
tion between the observed correlations and the
source dimensions. Some of these effects are il-
lustrated by considering Landau's hydrodynamical
model wherein each space-time point of the fluid
with temperature $T = T_c = m_\pi$ is taken as an indepen-
dent and chaotic emitting center with Planck
spectral distribution. In particular, this model
reproduces surprisingly well the observed $\pi-\pi$
and K-K correlations at the ISR.

1. INTRODUCTION

The correlation between identical particles produced
in a reaction is closely related to the space-time struc-
ture of the emitting source of these particles. This is the
base of Hanbury-Brown and Twiss method[1], used in radio-
astronomy to measure stellar dimensions, and also of the
GGLP effect[2] in nuclear physics. Several authors have
studied this phenomenon[3-7], but so far concrete applica-
tions have mostly been restricted to static sources, the
ones with factorized time and space dependences or field
theoretical model with a classical source[3]. While these
models clarify several qualitative features of the phenome-
non or even are convenient approximations in some cases, it
is questionable to straightforwardly apply their results
and try to extract from the data quantitative information
on more dynamical processes like hadronic interactions. In
these reactions, the particle sources typically move at
relativistic velocities with respect to each other and
important kinematical effects appear preventing us to es-
tablish a well known simple relation between the observed
correlations and the source dimensions.

In a previous paper[8], we gave a preliminary account
of our study of the identical-particle correlation, by
using Landau's hydrodynamic model as a prototype of such a
rapidly expanding particle source. Related discussions have
recently been made by some other authors[9] by using the
string-fragmentation model, which presents several common
features with the hydrodynamic models. In the present
paper, we shall give a more intuitive presentation of seve-
ral of the effects caused by the emission-source motions,
by considering a simple two-point-source model (Sec.2) and
then illustrating them by a more realistic hydrodynamical
model (Sec.3). For comparison with data, which will be a-
chieved in Sec.4, it is crucial to consider the emission of
quanta throughout the whole phase transition, during which
the energy density decreases from the initial value $\epsilon_{pl}(T_c)$,
calculated for the plasma phase, down to $\epsilon_h(T_c)$, computed
for the hadron gas. We will draw conclusions and propose
some experimental works in Sec.5.

2. TWO-POINT-SOURCE MODEL

Let us consider two point sources which are in move-

ment with respect to each other, so that when their space-time localizations are respectively given by $x'^\mu = (t', \vec{r}')$ and $x''^\mu = (t'', \vec{r}'')$, they independently emit quanta (pions). Two fixed counters A and B, placed at x_A^μ and x_B^μ are adjusted to detect particles in coincidence. Then, following the usual reasoning the amplitude of detecting two identical quanta, one with four-momentum $p_1^\mu = (E_1, \vec{p}_1)$ by A and another with $p_2^\mu = (E_2, \vec{p}_2)$ by B is given by

$$Amp \propto \exp\left\{i\left[p_1^\mu(x_{A\mu}-x'_\mu) + p_2^\nu(x_{B\nu}-x''_\nu)\right]\right\}$$
$$+ \exp\left\{i\left[p_1^\mu(x_{A\mu}-x''_\mu) + p_2^\nu(x_{B\nu}-x'_\nu)\right]\right\} \qquad (1)$$

and the probability

$$W(p_1, p_2) = |Amp|^2 \propto 2\left[1 + \cos(\Delta p^\mu \Delta x_\mu)\right], \qquad (2)$$

where

$$\Delta p^\mu = (\Delta E, \Delta\vec{p}) = (E_2 - E_1, \vec{p}_2 - \vec{p}_1) \qquad (3)$$

and

$$\Delta x^\mu = (\Delta t, \Delta\vec{r}) = (t'' - t', \vec{r}'' - \vec{r}'). \qquad (4)$$

The correlation coefficient is then written

$$C(p_1, p_2) = \frac{W(p_1, p_2)}{W(p_1)W(p_2)} = 1 + \cos(\Delta p^\mu \Delta x_\mu), \qquad (5)$$

where $W(p_i)$ is the single particle probability.

More generally, we are interested in two point sources that irradiate at random during a finite interval of time δt, so one has to integrate eq.(5) over t' and t'' with appropriate source-velocity dependent weight functions and some random phases. In general its explicit expression becomes complex, but for the sake of discussion here, we reinterpret our basic relation, eq.(5), by replacing it by a certain average

$$C(p_1, p_2) = 1 + \left\langle \cos(\Delta p^\mu \Delta x_\mu) \right\rangle. \qquad (5a)$$

In the static case, this equation establishes a direct connection between the two-identical-particle correlation and the distance Δr as well as the relative direction of the two point sources. Thus, by choosing $\Delta E = 0$ and measuring $C(p_1, p_2)$ at different values of $\vec{p} = (\vec{p}_1 + \vec{p}_2)/2$ and $\Delta\vec{p} = \vec{p}_2 - \vec{p}_1$, one easily determines $\Delta\vec{r}$. For moving sources, however, and especially when the velocities are variable, the problem becomes much more complex.

Let us first study two collinear point sources which move one away from the other along the x-axis. For simplicity, let us consider

$$\begin{cases} x'^\mu = (t', 0, 0, 0), \\ x''^\mu = (t'', x'', 0, 0), \end{cases} \qquad (6)$$

where the second source is accelerated and so with an increasing four-velocity $u_\mu = (u_0, u_1, 0, 0)$, each source having a half-life of δt as discussed below eq.(5). Let us try to measure the (longitudinal) distance between the two sources. It is clear from eq.(5a) that the most convenient way to achieve it is to place the two counters at $\sim 90°$, i.e., $\vec{p} \perp Ox$ (see Fig.1) and measure $C(p_1, p_2)$ as a function of $\Delta\vec{p} // Ox$ ($\Delta E = 0$). Now, x'' is changing here and so we do not have one distance but many of them. As is well known, if we assume that the spectral distribution is isotropic in the proper frame, in the laboratory frame it becomes

concentrated in the forward direction as u_1 increases. Hence, the larger the velocity u is, the smaller is its contribution to $\langle \; \rangle$ of eq.(5a) in the present case. This effect is the one which has been discussed also in Ref.9). The distance $\Delta x = x''$ that the correlation data reveal would then be the one corresponding to a "typical" u, obtained with the momentum spectrum as the weight function. To be more specific, let us assume that the invariant distribution is given by

$$E \frac{dn}{d\vec{p}} \propto u_\mu p^\mu exp\left[-\frac{u_\mu p^\mu}{T}\right] = u_0 E \, exp\left[-\frac{u_0 E}{T}\right]. \qquad (7)$$

Hence, we have

$$\langle u_0 \rangle \simeq \left(1 + \frac{2T}{E} + \frac{2T^2}{E^2}\right)\Big/\left(1 + \frac{T}{E}\right) \qquad (8)$$

with the corresponding rapidity width of $\Delta\alpha \simeq 0.94$, if $T \simeq m_\pi$ and $\langle p_T \rangle \simeq 0.35$ GeV, a number of the same order of magnitude as used in Ref.9). However, eqs.(7) and (8) show something more. If one calibrates the counters so as to detect large-momentum particles, $\langle u_0 \rangle$ decreases tending to 1, so $\Delta\alpha \to 0$. This means that if the second source is accelerated as happens in an expansion, the "effective" size which the correlation data show decreases as p_T increases.

Let us now study the measurement of the transverse "distances" between the source points (we are decomposing the vector $\Delta\vec{r}$ along three independent directions). For the configuration given by eq.(6), it is evident that such "distances" are identically zero, but in general x''^μ may have y'' and z'' components. To determine Δz, it is natural to put the detectors nearly parallel to the y-axis ($\vec{p} /\!/ Oy$), and measure $C(p_1,p_2)$ as a function of Δp_z ($\Delta E = 0$). To estimate Δy, one just turns the counters by $\pi/2$ and repeats the above procedure. One might think that it is also possible to evaluate Δy by setting the counters along the y-axis and measuring $C(p_1,p_2)$ as a function of Δp_y. However, for non-simultaneous emissions, i.e., $\Delta t = t''-t' \neq 0$, the argument of cosine in eq.(5a) becomes

$$\Delta p^\mu \Delta x_\mu = \Delta E \Delta t - \Delta p_y \Delta y$$

$$= \Delta p_y\left[\frac{\Delta E}{\Delta p_y}\Delta t - \Delta y\right] \xrightarrow[(\Delta y = 0)]{} \Delta p_y\left[\frac{\Delta E}{\Delta p_y}\Delta t\right]. \qquad (9)$$

So, although the actual Δy is zero for our two point sources given by eq.(6), it appears as if $\Delta y = -(\Delta E/\Delta p_y)\Delta t \simeq -v\Delta t$. In other words, when the second source emits, the field emitted by the first one has already travelled a distance $v\Delta t$, so the point $(t'',0,v\Delta t,0)$ behaves as an effective source simultaneously emitting with the second one. Evidently, the effect we are discussing here has nothing to do with the source motion, but just with the emission-time difference. However, such a delay in the emission time is a basic feature of any more realistic model of expanding objects and, as we will show later, it becomes crucial in the analysis of the data.

So far, we have restricted ourselves to the study of the correlation as a function of one component of $\Delta\vec{p}$, taking the other components equal to 0. Clearly, such configurations are highly improbable. This is a very important point when one tries to extract information on the source structure from the data, because if, say, the component of $\Delta\vec{p}$ which is parallel to $\vec{p}$ is $\neq 0$ and the correlation is seen as a function of a normal component of $\Delta\vec{p}$, for instance Δp_x, first it will not be $= 2$ at the origin ($\Delta p_x = 0$), but < 2 and also $\Delta p_x = 0$ will not be the point of maximum of $C(p_1,p_2)$. Obviously, this implies that a simple parametrization of the data by eq.(5a) or by a Bessel function as usually done in the case of a continuous source may lead to completely erroneous conclusions. To show these effects, let us again

consider the last example and now set the detectors so as to have $\vec{p} \,/\!/\, Oy$ and $\vec{\Delta p} = (\Delta p_x, \Delta p_y, 0)$, with $\Delta p_y > 0$ constant. Then, $\Delta p^\mu \Delta x_\mu = \Delta E \Delta t - \Delta p_x \Delta x$, which gives $\Delta p^\mu \Delta x_\mu > 0$ when $\Delta x = 0$ and $C(p_1, p_2) < 2$ there. The maximum of $C(p_1, p_2)$ is located at $\Delta p_x = \Delta E \Delta t / \Delta x > 0$.

3. HYDRODYNAMICAL MODEL

Let us now extend the discussion given in the preceding section to a more realistic extended source that we will describe by a variant of Landau model[10] in which we assume that the fluid is the quark-gluon plasma and the fireball mass is an event-dependent parameter. While the latter assumption is not necessary if we confine ourselves just to a theoretical study of the expansion effect on the correlation, it turns out to be essential when comparing the results with the existing data[11].

Since the final results are not expected to be very sensitive to the details of the expansion model, here we completely neglect the transverse expansion and use the asymptotic form of Khalatnikov solution[12], namely

$$\xi \equiv \ln \frac{T}{T_0} \simeq - c_0^2 \ln \frac{\tau}{\Delta} , \tag{10}$$

$$\alpha \simeq \frac{1}{2} \ln \frac{1+x}{1-x} \tag{11}$$

where

α = rapidity of the plasma,
c_0 = sound velocity $\cong 1/\sqrt{3}$ and
$\Delta = \sqrt{(1-c_0^2)/\pi}\,\ell$, 2ℓ = initial thickness of the fireball

This solution is valid when $|\xi| \gg |\alpha|$.

Usually, one assumes that the final particles appear

when the local temperature reaches a certain critical value $T = T_c \cong m_\pi$, which defines a transition surface. However, due to the statistic factor, which is large in the q-g plasma, its energy density $\epsilon_p(T_c)$ is too high to assume that pions appear from such a surface. We think it is more reasonable to let the fluid expand further and assume that the final-particle emission occurs during this interval of time when the energy density goes down to the characteristic value for the hadronic gas $\epsilon_h(T_c)$. Since the pressure remains constant during the transition, the expansion in this stage is expected to be inertial, being α in eq.(11) unchanged. Here, we shall first study the problem under the assumption that particles are emitted at $\tau = \tau_c$, when $\epsilon = \epsilon_p(T_c)$ and then improve the results in the next section, by considering the above effect, but for simplicity taking $\tau = \langle \tau \rangle \propto \tau_c$, where $\langle \tau \rangle$ is a certain average value which will be computed later. Evaporation from the hot plasma would certainly exist but here we assume that the bulk of the produced particles come from the transition region which develops from inside to outside. The effects of resonance production, final state interactions[3], as well as of the partial coherence of the source[3,7], if any, should be taken into account, but here we simply consider a totally chaotic source, which will show (Sec. IV) surprisingly well fitted to reproduce the existent data.

So, let us initially assume that each point of the surface $\tau = \tau_c$ in the plasma where $T = T_c \cong m_\pi$ is an independent chaotic source with the momentum spectrum

$$f(p) \simeq \frac{1}{(2\pi)^3} \frac{u^\mu p_\mu}{E} \exp\left(-\frac{u^\mu p_\mu}{T_c}\right) , \tag{12}$$

where

$$\begin{cases} u^\mu = (\text{ch}\alpha, \text{sh}\alpha, 0, 0) = \text{4-velocity of the fluid,} \\ p^\mu = (E, p_x, p_y, p_z) = \text{4-momentum of an emitted} \\ \qquad\qquad\qquad\qquad\qquad\qquad \text{particle.} \end{cases} \tag{13}$$

The amplitude for finding a particle at x and emitted at x' is written

$$J(x,x') = \int d\vec{p}\,\sqrt{f(p)}\,\exp\left[-i p_\mu (x^\mu - x'^\mu)\right]\exp\left[i\,\theta(x')\right]\,, \quad (14)$$

where $\theta(x')$ is a random phase. Following the notation of Ref.5), the probability of detecting two quanta of momenta p_1 and p_2 in an event is

$$W(p_1,p_2) = \tilde{I}(0,p_1)\tilde{I}(0,p_2) + \left|\tilde{I}\left[p_1-p_2,\tfrac{1}{2}(p_1+p_2)\right]\right|^2\,, \quad (15)$$

where

$$\begin{cases} \tilde{I}(\Delta p, p) = \int dx\, d\Delta x\, \exp\left[ix\Delta p + i\Delta x\, p\right]\int dx'\, I(x,\Delta x, x')\,, \\ \left\langle J^*(x-\tfrac{\Delta x}{2}, x')\, J(x+\tfrac{\Delta x}{2}, x'')\right\rangle = \delta(x'-x'')\, I(x,\Delta x, x') \end{cases} \quad (16)$$

and the average is taken over the random phases $\theta(x')$ and $\theta(x'')$. We also have

$$W(p_i) \equiv \left\langle \left|\int dx'\int \exp(i p_i x)\, J(x,x')\, dx\right|^2\right\rangle = \tilde{I}(0,p_i)\,. \quad (17)$$

Thus, by inserting eqs.(12-14) into (16) and then $I(\Delta p, p)$ so obtained into eqs.(15) and (17), we can easily calculate the correlation coefficient $C(p_1,p_2)$ defined by eq.(5), giving

$$C(p_1,p_2) = 1 + \frac{4\left[J_1(R\Delta p_T)\right]^2}{T_c\, R^2 \Delta p_T^2}$$

$$\exp\left\{-2\left[\sqrt{\left(\frac{E^2-p_L^2}{2T_c^2} - \frac{\Delta E^2-\Delta p_L^2}{2}\tau_c^2\right)^2 + \left(E\Delta E - p_L\Delta p_L\right)^2\frac{\tau_c^2}{T_c}} + \frac{E^2-p_L^2}{2T_c^2} - \frac{\Delta E^2-\Delta p_L^2}{2}\tau_c^2\right]^{\frac{1}{2}}\right\}$$

$$\times \frac{}{\left[\left(\frac{E^2-p_L^2}{T_c^2} - (\Delta E^2-\Delta p_L^2)\tau_c^2\right)^2 + 4\left(E\Delta E - p_L\Delta p_L\right)^2\frac{\tau_c^2}{T_c^2}\right]^{3/4}}$$

$$\exp\left\{\frac{1}{T_c}\left[\sqrt{E^2-p_L^2 + \frac{\Delta E^2-\Delta p_L^2}{4} + (E\Delta E - p_L\Delta p_L)} + \sqrt{E^2-p_L^2 + \frac{\Delta E^2-\Delta p_L^2}{4} - (E\Delta E - p_L\Delta p_L)}\right]\right\}$$

$$\times \frac{}{\left[\left(E^2-p_L^2 + \frac{\Delta E^2-\Delta p_L^2}{4}\right)^2 - \left(E\Delta E - p_L\Delta p_L\right)^2\right]^{1/4}}$$

$$\times \left\{\left[\left(\frac{E^2-p_L^2}{T_c}\right)^2 + \left(\frac{E\Delta E - p_L\Delta p_L}{2T_c}\right)^2 + \left(E\Delta E - p_L\Delta p_L\right)^2\tau_c^2 + \frac{(\Delta E^2-\Delta p_L^2)^2}{4}\tau_c^2\right]\right.$$

$$\left. - \left[\frac{E^2-p_L^2}{T_c} + (\Delta E^2-\Delta p_L^2)\tau_c^2\right]^2 \left(E\Delta E - p_L\Delta p_L\right)^2\right\}^{1/2}\,, \quad (18)$$

where

$$\begin{cases} p \equiv \tfrac{1}{2}(p_1+p_2) = (E, p_L, p_y, p_z)\,, \\ \Delta p \equiv p_1 - p_2 = (\Delta E, \Delta p_L, \Delta p_y, \Delta p_z) \\ \Delta p_T = \sqrt{\Delta p_y^2 + \Delta p_z^2}\,. \end{cases} \quad \text{and} \quad (19)$$

We fix the critical temperature $T_c = m_\pi$ and τ_c shall be determined by imposing the condition $T=T_c$ on the plasma. To doing so, we need the initial temperature T_0, which depends on the mass M of the fireball and its initial size. It has been shown that the hypothesis of large mass Lorentz contracted fireball formation around one or both of the incident particles provides a nice framework to accounting for several of the experimentally observed quantities[13,14]. In Ref.14), it has been shown that, if such a fireball is made of quarks and gluons, a very reasonable choice of the initial radius $R = R_{proton}$ leads to the experimentally observed mean charged multiplicity $\langle N_{ch}\rangle(M)$ as well as to the pseudo-rapidity distribution $d\sigma/d\eta$ (M), which have recently been

measured in large-mass diffractive dissociation at the $\bar{p}p$ collider[15]. In contrast, if such a fireball is made of pions, a too large radius R becomes necessary to fitting the data. It would also be possible to impose some other initial conditions wherein non constant space-time distributions of temperature and velocity are specified[16,17], but in this case we would not have a definite principle for such an assignment and, moreover, a simple version in which T and v are specified on a hyperbola τ = const. gives exactly the same asymptotic Khalatnikov's solution; so, as far as the practical results are concerned, we can go backward in time and start from a constant temperature $T=T_o$ and v=0 at t=0. Then, following Ref.14),

$$T_o = \left[\frac{45}{4\pi^3 m_p R^3 \left(g_g + \frac{7}{8} g_q\right)}\right]^{1/4} \sqrt{M} = b\sqrt{M} \simeq 0.118\sqrt{M} , \quad (20)$$

where g_g and g_p are the statistical weights of gluons and quarks respectively and the numerical value of b in the last equality has been fixed (in $GeV^{1/2}$), by using the fit $\langle N_{ch} \rangle \equiv 1.8\sqrt{M}$ (which means R=0.76 f if N_f=2 as is taken throughout this Section). Then, from eq.(10) we have

$$\tau_c^2 = \Delta^2 \left(\frac{T_o}{T_c}\right)^6 = \frac{8 m_p^2}{3\pi}\left(\frac{b}{m_\pi}\right)^6 \left(R^2 M\right) \simeq 3.88 M . \quad (21)$$

We shall now illustrate the kinematical effects discussed in Sec.II, by using eq.(18) above. Let us first consider two equal energy quanta emitted symmetrically with respect to some transverse direction and plot $C(p_1, p_2)$ as a function of $\Delta p = |\vec{p}_2 - \vec{p}_1|$. We show in Fig.2, curves with Δp_L=0 and Δp_T=0 at two different values of M. In the Δp_L=0 case ($\Delta p = \Delta p_T$), the correlation coefficient does not show any M dependence because the transverse dimensions remain constant in the present version and independent of the energy. On the other hand, in the Δp_T=0 case ($\Delta p = \Delta p_L$), a strong M dependence of $C(p_1, p_2)$ does appear. This effect can easi-

ly be understood if we notice that according to eqs.(10) and (11) the surface $T=T_c$ from which the hadrons emerge is a hyperbola which moves upward as the mass M increases (see Fig.3) and curves with constant velocities are straight lines starting from the origin of the coordinate frame O, namely x=vt, which means as discussed before that the correlation in Δp_L decreases (apparent size increases) with M.

Let us now study the p_T dependence of the correlation. We show in Figs.4 two families of curves corresponding to two different arrangements of counters, each curve computed with a fixed average transverse momentum p_T of the two quanta. Their average direction has been set to be $\pi/2$ with respect to the longitudinal axis and the curves in Fig.4a represent the longitudinal-momentum correlation whereas those in Fig.4b correspond to the one with $\Delta \vec{p} // \vec{p}$ (source-depth measurement). In both the cases, one clearly sees that as p_T increases the width of $C(p_1, p_2)$ increases as well, mimicking a diminution of the effective source size, in agreement with our previous discussion in Sec.II.

It is also interesting to see the fireball-mass dependence of the correlation coefficient as a function of Δp_y as displayed in Fig.5 (the axes have been chosen as in Fig.1a, where the fireball expands along the x-axis). For all these curves the transverse dimensions of the source are the same, difference occurring only in the longitudinal expansion. As discussed in Sec.II (eqs.(7) and (8) and below), once the average energy of the identical particles is fixed, the average velocity of the effective source $\langle u \rangle$ is also defined. Now, by looking at Fig.3 one notes that for the same velocity of the fluid the time Δt becomes larger as M increases, yielding due to eq.(9) larger apparent depth for the source or narrower curve for $C(p_1, p_2)$).

Let us now examine some more probable cases of $\Delta \vec{p}$ dependence of the correlation, in which more than one component of $\Delta \vec{p}$ are $\neq 0$. Figure 6 displays some examples where

the correlation has been computed at an average direction of $\pi/2$ with respect to the symmetry axis and with $\Delta p_y \neq 0$. In each case, $C(p_1, p_2)$ is plotted as a function of $\Delta p'$, where $\Delta p' = (\Delta\vec{p}^2 - \Delta p_y^2)^{1/2}$. The main feature of these curves is as seen the fact that $C(p_1, p_2) < 2$ at the origin $\Delta p' = 0$, which is quite natural since here $\Delta p' = 0$ does not implies $\Delta\vec{p} = 0$. As we have already discussed it in the last Section (and here we emphasize it again) data are never obtained with, say, $\Delta p_y = 0$, but within a certain limit, so <u>the experimentally measured correlation coefficient is always smaller than 2, even if the source is totally chaotic</u>. Also, the maximum of $C(p_1, p_2)$ is not necessarily at $\Delta p' = 0$. Although this is the case for the curves in Fig.6, this feature can more clearly be seen when one looks at Fig.7, where we show $C(p_1, p_2)$ as a function of Δp_x when $\Delta p_y \neq 0$ and the average direction of the two quanta are not at right angle with respect to the expansion axis ($p_L \neq 0$).

4. COMPARISON WITH DATA

In the last Section, we have shown several kinematical effects that the source expansion causes on the correlation by considering a hydrodynamical model where the source is a quark-gluon plasma which is assumed to be formed during a hadronic collision and which emits the observed pions as it cools by expansion and reaches the critical temperature $T_c \equiv m_\pi$. As has been mentioned there, due to the large statistical factor in the q-g plasma, its critical energy density $\epsilon_p(T_c)$ is much higher than the characteristic hadronic energy density $\epsilon_h(T_c)$. Then, in order to compare the results with the data[11], a more realistic model is needed, whereby the fluid expands further undergoing a phase transition. Particle emission occurs during this time interval in which the energy density decreases from $\epsilon_p(T_c)$ down to $\epsilon_h(T_c)$.

In estimating the correlation coefficient with the phase transition taken into account, we assume following Gyulassy and Matsui[18] that an isentropic path is followed during such a transition. Then, because our fluid is one-dimensional (with the transverse expansion neglected) and is expected to undergo an inertial expansion during this stage as argued in Sec.3, the fluid velocity remains v=x/t =constant and

$$\Delta\tau = s_p \tau_p = s_h \tau_h , \quad (\tau_p \leq \tau \leq \tau_h) \tag{22}$$

where s_p and τ_p are respectively the entropy density and the (proper) time when the transition begins and s_h and τ_h are the same quantities at the end of the transition. We assume the entropy density s_p as being the one of a (massless) non-interacting quark-gluon plasma

$$s_p = g_p \frac{2\pi^2}{45} T_c^3 , \tag{23}$$

with the effective number of freedom $g_p = 2\times8 + 7\times(2\times3\times2\times N_f)/8$, being N_f the number of quark flavors, and s_h as that of the usual pion+kaon ideal gas, namely

$$s_h = \frac{1}{2\pi^2}\left[g_\pi G(z_\pi) + g_K G(z_K) \right] T_c^3 , \tag{24}$$

where $g_\pi = 3$, $g_K = 4$, $z_i = m_i/T_c$ and

$$G(z) = z^2 \sum_{n=1}^{\infty} \frac{4 K_2(nz) + nz K_1(nz)}{n^2} . \tag{25}$$

So, with the use of eqs.(20) and (21) (the numerical value of b has now to be changed to 0.099 because our hadronic gas contains kaons as well as pions), we get

$$\tau_h = \frac{s_p}{s_h} \tau_c = \frac{(4\pi^4/45) g_p}{g_\pi G(z_\pi) + g_K G(z_K)} \tau_c , \tag{26}$$

where $G(z_\pi = 1) \approx 7.476$, $G(z_K = 3.5) \approx 2.156$ and τ_c is given by eq.(21).

At a given instant of time in the interval $\tau_p \leqslant \tau \leqslant \tau_h$, we have

$$s = f \, s_p + (1-f) s_h, \qquad 0 \leqslant f \leqslant 1 \tag{27}$$

i.e., the total entropy density of the fluid is a sum of a plasma portion and a hadronic portion, so that $s=s_p$ at $\tau = \tau_p$ and $s=s_h$ at $\tau = \tau_h$. It immediately follows that

$$f = \frac{\tau_h - \tau}{\tau_h - \tau_p} \cdot \frac{\tau_p}{\tau}, \tag{28}$$

which is the fraction of the mixture that is still in the plasma phase. We think this portion of the entropy, namely

$$s_f \equiv f \, s_p = \frac{\tau_h - \tau}{\tau_h - \tau_p} \cdot \frac{\tau_p s_p}{\tau} \tag{29}$$

(in terms of density) should properly considered as the particle-emission source during the transition.

So, a more exact calculation of $C(p_1, p_2)$ would amount to including the factor given in eq.(29) into eq.(12) or (16) of the previous Section, where the integration has been simplified by $\delta(\tau - \tau_c)$ assumed there. However, as will be discussed below this is not all the story. In order to get quantities comparable with the data[11], more integrations or averaging processes are required. In the present paper, we instead preferred to simplify the problem and estimate $C(p_1, p_2)$ by considering "typical" values of all these integration variables and computing it there. Thus, instead of performing a detailed τ integration in eq.(16)* with an additional factor f given by eq.(28), we have com-

---

*See details in Ref.8).

puted the average time

$$\langle \tau \rangle = \frac{\frac{1}{2}\left(\frac{\tau_h}{\tau_c} - 1\right)^2}{\frac{\tau_h}{\tau_c}\left[\ln \frac{\tau_h}{\tau_c} - 1\right] + 1} \cdot \tau_c \tag{30}$$

with s_f taken as the weight function and then replaced τ_c by $\langle \tau \rangle$ in eq.(18). In Table I, we show the numerical estimates for τ_h / τ_c and $\langle \tau \rangle / \tau_c$ when $N_f = 2$ or 3 and the hadron gas is made of pions and kaons.

Now, as stressed at the end of Sec.3, we should not forget that the kinematical situations chosen there are highly ideal. Due to the low statistics, the available correlation data have been obtained by considering pairs of identical particles in much wider kinematical domains. For instance, in Ref.11), data were obtained for pp collisions at $\sqrt{s} = 53$ GeV, by detecting all π^+ mesons with $p_T \gtrsim 0.1$ GeV and in the rapidity range of $|y| \lesssim 1.0$. Then, the correlation of such pions is determined by taking all the pairs into account and as a function of q_L, with $q_T \lesssim 0.15$ GeV or as a function of q_T, with $q_L \lesssim 0.15$ GeV. Here, q_L (and q_T) are the usual Kopilov's variables[4], namely, the components of $\Delta \vec{p}$ which are parallel (and orthogonal) to $\vec{p} = (\vec{p}_1 + \vec{p}_2)/2$.

Thus, in order to make comparisons with experimental data, we should average our result given by eq.(18) over several of the kinematical variables. However, inclusion of all this averaging procedures makes the computation much more complex, so for the sake of simplicity we decided to invert it and estimate $C(p_1, p_2)$ by adopting some "typical" (=average) values of all the variables but one, namely q_T or q_L, as function of which the data are given. The only averaging which has explicitly been carried out is the one over the azimuthal angle with respect to the "typical" momentum $\vec{p}$ taken from data.

We present the results of this valuation in Figs.8

and 9, together with the data of Ref.11). As it can be seen the agreement is quite good and especially in Fig.8a) one sees that, although our source is <u>completely chaotic</u>, q_T dependence of $\langle C(p_1,p_2)\rangle$ for $\pi^+\pi^+$ is much better reproduced by our curves than by the empirical fit presented there. Observe that we have not adjusted any parameter by fitting the data, but all the numerical parameters have been predetermined either by the experimental conditions described in Ref.11) or by theoretical considerations (as $T_c \cong m_\pi$ and g_p). It is interesting to notice that no appreciable diference in $\langle C(p_1,p_2)\rangle$ is introduced by changing the number of quark flavors. This is, in our opinion, due mostly to the fact that the data are the average over several pion-momentum directions, so that mainly those pairs which are relatively insensible to the collective motions give contributions to the data. We think that in analyzing data if one enhances the longitudinal (Δp_L) correlation, one can better discriminate among several possibilities.

5. CONCLUSIONS

We have studied in the present paper several kinematical effects which a rapid expansion of the source may cause on the correlation between two identical particles emitted in a high energy hadronic collision. This has been schematized by a simple two-point-source model in Sec.2 and then extended to a continuous chaotic source in Sec.3, by using the scaling solution of the hydrodynamical equations as such a source.

We have shown that what we actually measure in correlation experiments are the source dimensions characterized by some typical collective four-velocity $u_o \lesssim \langle u_o \rangle$. Numerically, if $\langle p_T \rangle \cong 0.35$ GeV, such an interval turns out to be, in terms of rapidity of the source points $\Delta \alpha \cong 1$. This value,

however, depends on p_T and decreases as p_T increases, suggesting an experimental study of the velocity distribution of the source.

The q_L dependence of the correlation coefficient does not directly show the source depth but a combined effect of the depth and the emission time interval, both in the velocity interval mentioned above. This effect may be used in high-energy heavy-ion collisions in order to discriminate between single-source- and multi-source-formation mechanisms.

Experimentally, all the components of p are generally non-zero. Thus, e.g., $q_T = 0$ if one is plotting $C(p_1,p_2)$ as a function of q_L. It follows that <u>the experimental $C(p_1,p_2)$ is always smaller than 2 at the origin ($q_L = 0$) without implying necessarily that the source be coherent</u>. In this paper, we have taken a completely chaotic source which has shown to be enough to reproducing the data.

The correlation is shown to be strongly dependent on the mass M of the fireball. By varying the incident energy $\sqrt{s}$, one may experimentally study its average mass $\langle M \rangle$ dependence. In Figs.10 and 11 we show some predictions for such an energy dependence of $\pi^+\pi^+$ (or $\pi^-\pi^-$) correlation at the $\bar{p}p$ collider energies, by assuming exactly the same kinematical restrictions imposed in Ref.11). As is seen, there appears a strong energy dependence of $\langle C(p_1,p_2)\rangle$ as one goes from the ISR to the collider energies. It is also desireable to see how it varies with M at a fixed energy, because it is well known that there is a large inelasticity fluctuation in hadronic collisions.

In comparing with the data, we have assumed formation of quark-gluon plasma which undergoes a (first-order) transition as it freezes down to a critical temperature. The agreement with data is quite good suggesting that the physical idea behind our model is reasonable. As a first estimate, we have simplified the computation by replacing

the average values of $C(p_1, p_2)$ by its values at the average points. We intend to improve the results in the near future by effectively carrying several integrations out. Nevertheless, our feeling is that the explicit integration does not change the main features of the results.

The averaging over several kinematical variables washes out many of the interesting features of two-particle correlation. This is especially well illustrated by Figs.2 and 6. Although it may be an arduous task to get statistically reliable data, it is worthwhile to narrow down the kinematical windows, for it will certainly give a much richer information on the space-time structure of the hadronic collisions.

In short, we conclude that in high-energy hadronic interferometry, we cannot get any correct information neither about the nature of the source nor about its dimension without taking the source expansion effects into account.

REFERENCES

1) R.Hanbury-Brown and R.Q.Twiss, Phil.Mag. 45,663(1954); Nature 178,1046(1956).

2) G.Goldhaber, S.Goldhaber, W.Lee and A.Pais, Phys.Rev. 120,300(1960).

3) M.Gyulassy, S.K.Kauffmann and L.W.Wilson, Phys.Rev. C20 2267(1979).

4) G.I.Kopilov and M.I.Podgoretzky, Sov.J.Nucl.Phys. 14, 604(1972); 15,219(1972); 18,336(1974).
G.I.Kopilov, Phys.Lett. 50B,472(1974).
M.I.Podgoretzky, Sov.J.Nucl.Phys. 37,272(1983).

5) E.V.Shuryak, Phys.Lett. 44B,387(1973).

6) G.Cocconi, Phys.Lett. 49B,459(1974).

7) G.N.Fowler and R.M.Weiner, Phys.Lett. 70B,201(1977).

8) Y.Hama and Sandra S.Padula, "Bose-Einstein Correlation in Landau's Model", II International Workshop on Local Equilibrium in Strong Interaction Physics, Santa Fe (USA), April 9-12, 1986.

9) B.Andersson and W.Hofmann, Phys.Lett. 169B,364(1986).

10) L.D.Landau, Izv.Akad.Nauk SSSR Ser.Fiz. 17,51(1953); Collected papers, ed. D.Ter Haar (Pergamon,Oxford,1965) p. 569.

11) Axial-Field-Spectrometer Collab., T.Akesson et al., Phys. Lett. 129B,269(1983); 155B,128(1985).

12) I.M.Khalatnikov, Zhur.Eksp.Teor.Fiz. 26,529(1954).

13) Y.Hama, Phys.Rev. D19,2623(1979);
Y.Hama and F.W.Pottag, Rev.Bras.Fís. 12,247(1982);
Y.Hama and F.S.Navarra, Phys.Lett. 129B,251(1983); Z. Phys. C26,465(1984).

14) Y.Hama and F.W.Pottag, "Diffractive Excitation of the Quark-Gluon Plasma", in preparation for publication.

15) UA4 Collaboration, D.Bernard et al., Phys.Lett. 166B, 459(1986).

16) J.D.Bjorken, Phys.Rev. D27,140(1983).

17) K.Kajantie and L.McLerran, Phys.Lett. 119B,203(1982).

18) M.Gyulassy and T.Matsui, Phys.Rev. D29,419(1984).

Table I

N_f	R	τ_h/τ_c	$\langle \tau \rangle/\tau_c$	τ_c(at M=40 GeV)
2	0.95 f	10.32	2.94	1.83 f
3	0.88 f	13.24	3.41	1.70 f

Numerical estimates of R, τ_c (at M=40 GeV), τ_h/τ_c and $\langle \tau \rangle/\tau_c$, under the assumption of pion+kaon gas at the final state.

FIGURE CAPTIONS

Fig.1: A schematical representation of relatively moving two point sources. A graphical definition of the vectors $\vec{p}$ and $\Delta\vec{p}$ are also shown.

Fig.2: Correlation parameter given by eq.(18), as a function of $\Delta p = |\vec{p}_1 - \vec{p}_2|$, when $\vec{p}_1$ and $\vec{p}_2$ are symmetrical with respect to some transverse direction. The coordinate axes have been chosen as in Fig.1, with Ox parallel to the expansion direction, $\Delta p_L \equiv p_x$. The curves labeled <u>average</u> correspond to the mean values taken over the azimuthal angle with respect to $\vec{p}$.

Fig.3: Graphical representation of the transition surface $T=T_c$ (or $\tau=\tau_c$) for two different values of the fireball mass M. The straight line indicates the curve v-const.

Fig.4: p_T dependence of the correlation coefficient a)as a function of Δp_L at M-40 GeV and b) as a function of Δp_T at M=540 GeV.

Fig.5: Fireball mass dependence of the correlation coefficient as a function of Δp_y.

Fig.6: Correlation coefficient with $\Delta p_y \neq 0$, as a function of $p' = (\Delta p_x^2 + \Delta p_z^2)^{1/2}$.

Fig.7: Correlation coefficient with $\Delta p_y \neq 0$ and $p_L \equiv p_x \neq 0$, as a function of $\Delta p_L \equiv \Delta p_x$.

Fig. 8: Average $\pi^+\pi^+$ correlation coefficient, computed as explained in the text, is compared with the experimental data[11]. The continuous curves are our estimates with $N_f = 3$ ($g_p = 47.5$), the broken lines with $N_f = 2$ ($g_p 37$), whereas the dashed lines are the empirical fits given in Ref.11). In accordance with the experimental conditions, we have taken $\langle M \rangle = 37.5$ GeV, $\langle p_T \rangle = 0.38$ GeV, $\langle \theta \rangle = 1.01$ rad and in a) $\langle q_L \rangle = 0.075$ GeV and in b) $\langle q_T \rangle = 0.1$ GeV.

Fig. 9: Average KK correlation coefficient, computed as explained in the text, is compared with the experimental data[11]. The symbols are the same as those ones employed in Fig.8. Following the experimental conditions, we have taken $\langle M \rangle = 40$ GeV, $\langle p_T \rangle = 0.44$ GeV $\langle \theta \rangle = 0.85$ and $\langle q_L \rangle = 0.15$ GeV.

Fig.10: Energy dependence of the average $\pi^+\pi^+$ correlation coefficient as a function of q_T, computed under the assumption of the same kinematical restrictions as in Ref.11).
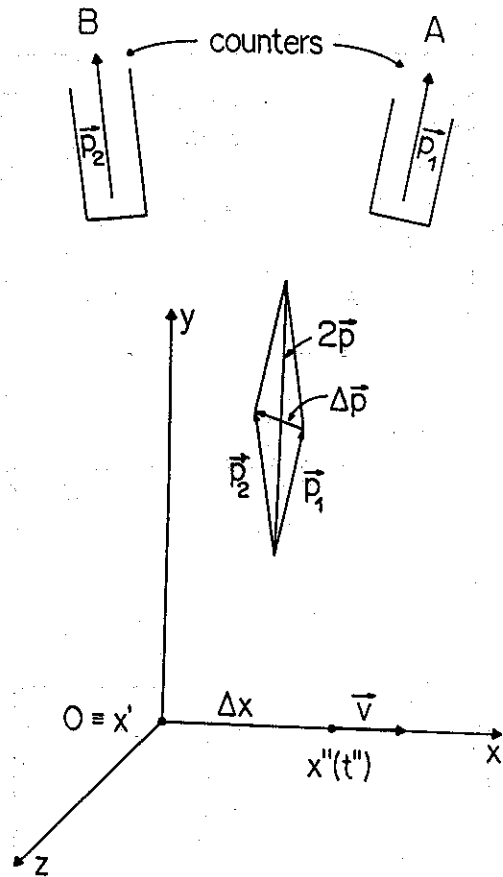
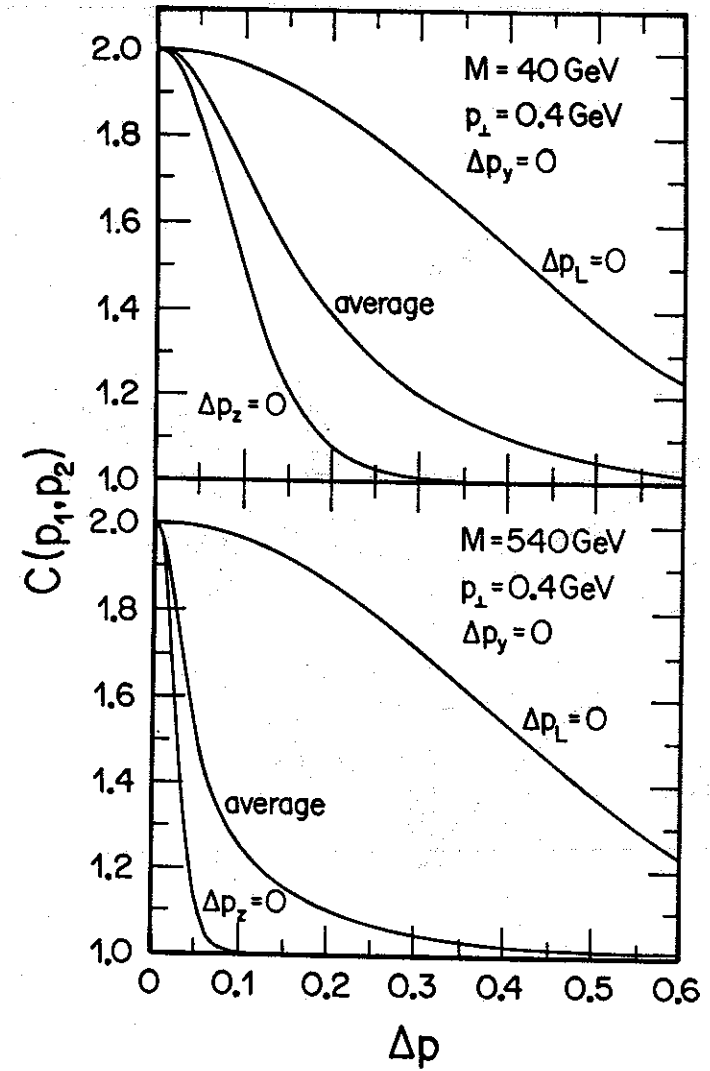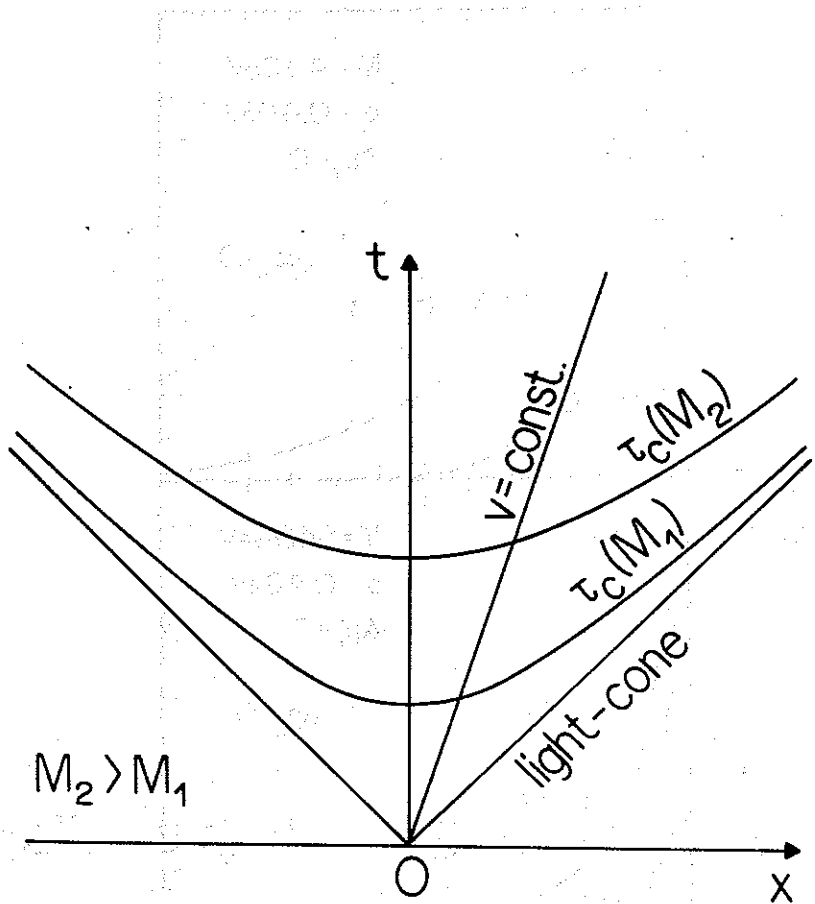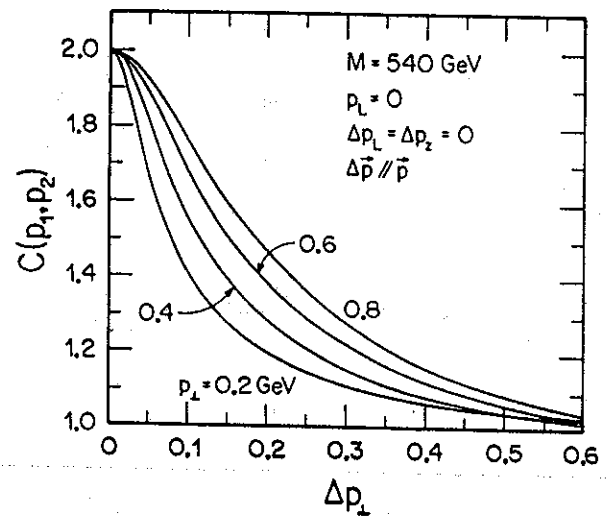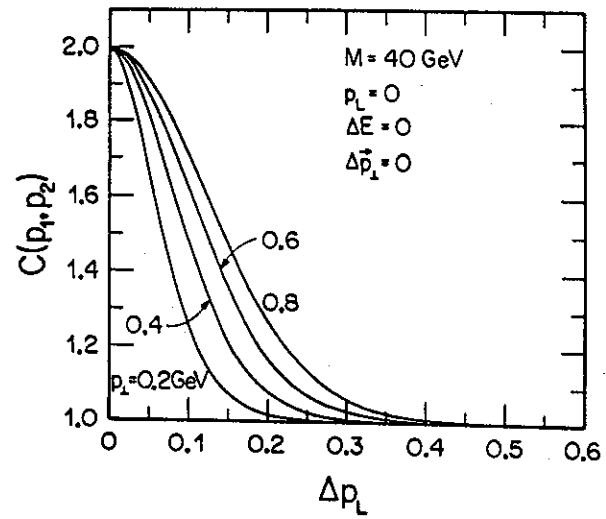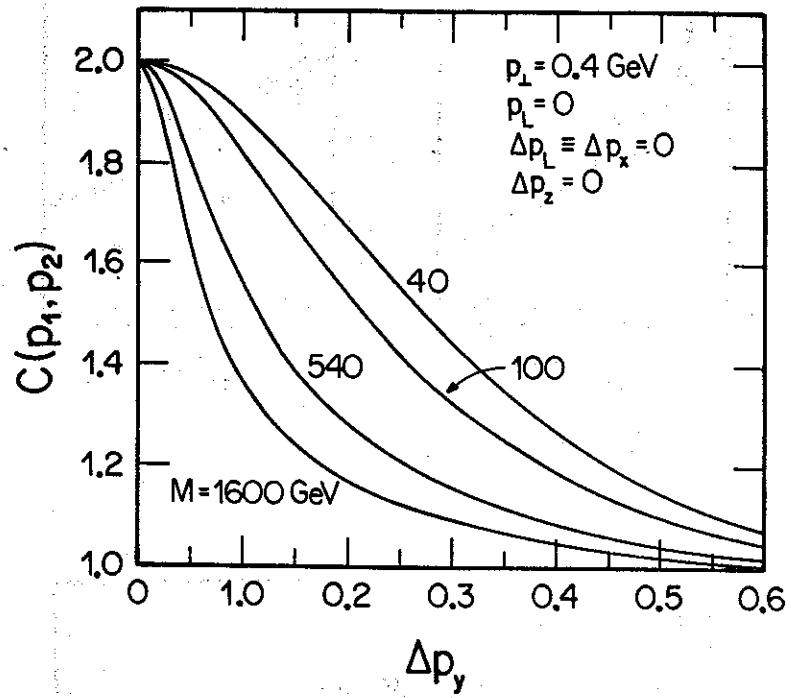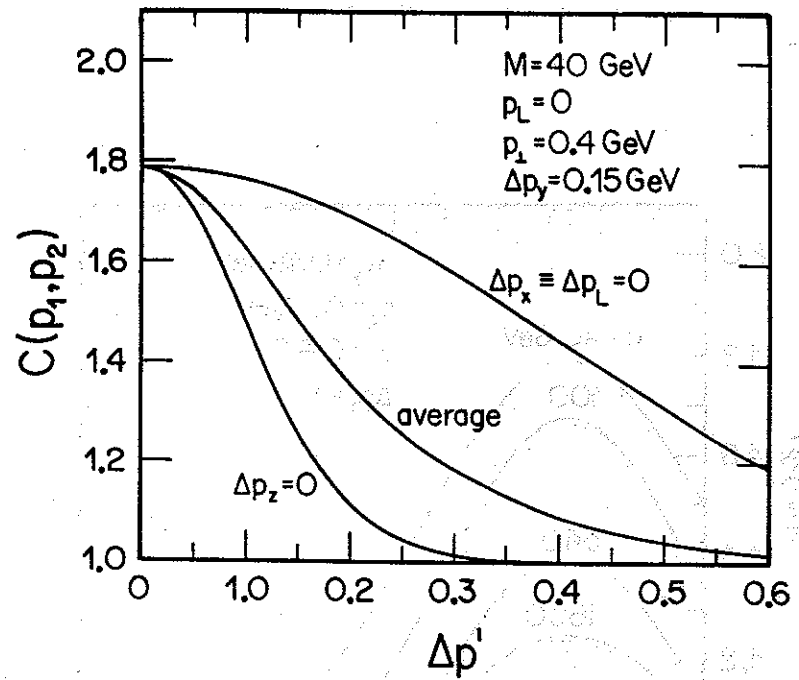Fig.11: The same as in Fig.10, but as a function of q_L.
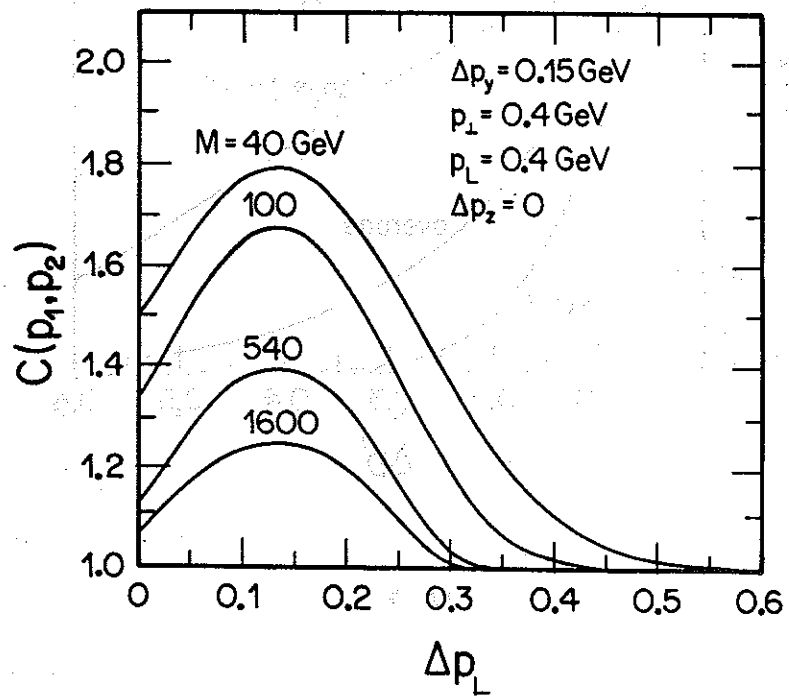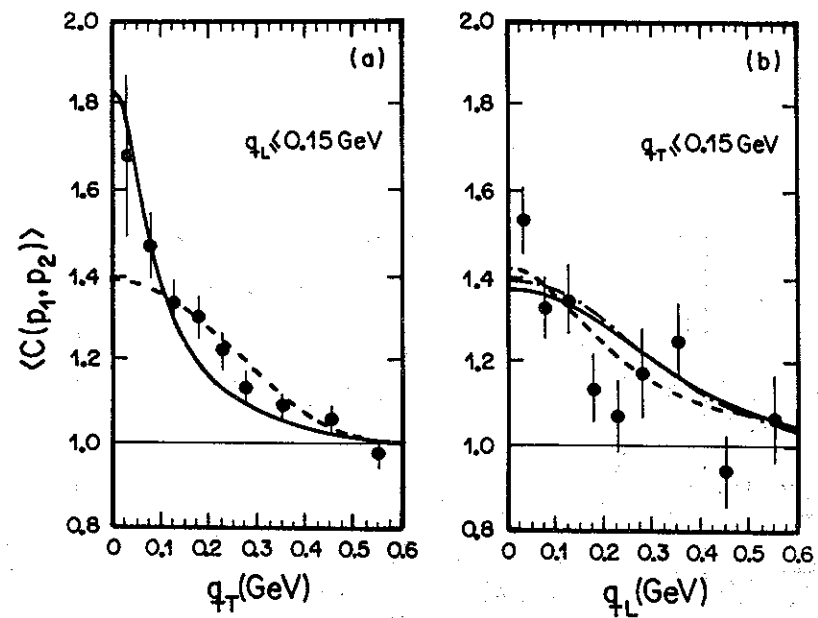
Fig. 1

Fig. 2

Fig. 3

Fig. 4

Fig. 5

Fig. 6

Fig. 7

Fig. 8

Fig. 9

Fig. 10

Fig. 11